Supplementary Figures

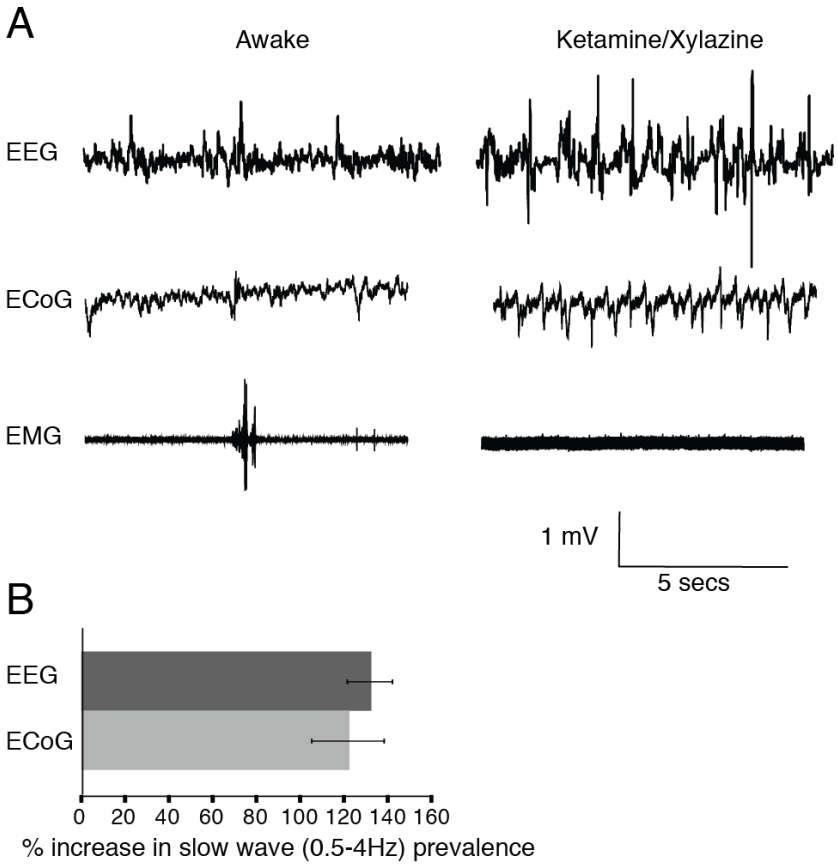

Fig. S1. Validation of Sleep/Wake Scoring

Standard EEG electrodes are fairly large (1-2 mm) and rest on top of the dura. To avoid interference with CSF convective fluxes in the subarachnoid space due to placement of EEG electrodes, ECoG was recorded in combination with EMG in all in vivo 2-photon imaging experiments. To evaluate how accurately ECoG/EMG recordings detect transitions in the arousal state, standard EEG recordings were compared to cortical ECoG recordings obtained in the same animals. (**A**) Standard EEG electrodes were positioned over the left hemisphere (2.5 mm lateral and 2 mm posterior to bregma) the day before the experiments. ECoG recordings were collected by inserting a glass micropipette 150 µm below the pial surface in the right hemisphere (2.5 mm lateral and 2 mm posterior to bregma). The EMG electrode was inserted in the neck muscles. (**B**) Comparison of percentage increase in slow wave prevalence upon transition from awake to ketamine/xylazine anesthesia using standard EEG electrodes and ECoG recordings (n = 5).

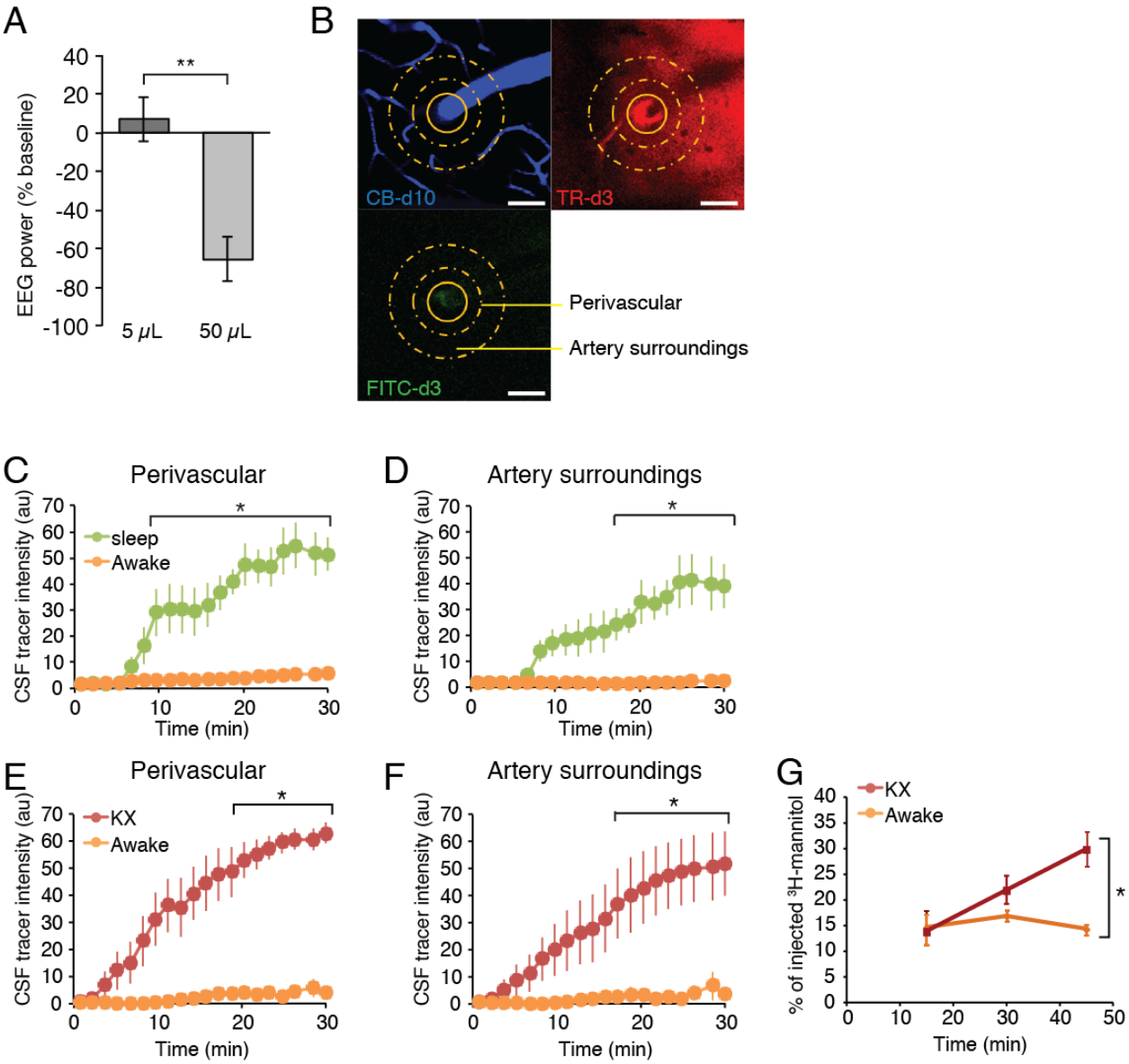

Fig. S2. Effect of intracisternal injection on ECoG and comparison of perivascular and parenchymal CSF tracer influx in two different arousal states in the same animal.

(A) Analysis of the effect of intracisternal injection of artificial cerebrospinal fluid on (aCSF) ECoG power. The aCSF contained TR-d3 and FITC-d3 (both 5%) and was injected at a rate of 1 µl/min. Injecting 5 µl was not associated with changes in EcoG power, whereas the 50 µl injections triggered a transient dampening of ECoG signal amplitude (*P < 0.05 One-Way ANOVA with Tukey Post hoc test). **(B)** To establish the effect of the arousal state on CSF tracer influx kinetics, Texas red or FITC labeled dextran with identical molecular weight (3kD) were injected in cisterna magna in the same animal during two different arousal states. We

compared the influx of Texas red (TR-d3) and FITC (FITC-d3) dextran in sleeping mice and then again after waking them up by gentle movement of their tail. These experiments were done when mice are naturally asleep (12-2pm). In another group of mice, tracer influx in awake mice was compared to tracer influx after the mice were anesthetized with ketamine/xylazine. These experiments were performed when mice were naturally awake (8-10pm). Tracer influx was analyzed along peri-arterial pathways and in the cortical parenchyma using in vivo 2-photon laser scanning microscopy through a closed cranial window. The cerebral vasculature was visualized via intravenous injection of Cascade Blue-dextran-10 (CB-d10) and penetrating arterioles were identified by morphology and the flow pattern: surface arteries passed superficially to surface veins and exhibited less branching at superficial cortical depths. The Image analysis of intracisternal tracer penetration was conducted with ImageJ software (NIH) with the UCSD plugin set. Imaging planes 100 µm below the cortical surface were selected for the analysis. To define peri-arterial tracer movement, a circular region of interest (ROI, 25 pixels in diameter) was defined surrounding penetrating arteriole (yellow solid circle). To define tracer movement into peri-arterial brain tissue, a donut-shaped ROI was defined that had an external diameter of 150 pixels and an internal diameter of 50 pixels (thus excluding the paravascular ROI, yellow dashed donuts) (*3*). Both circles were centered around penetrating arterioles. Scale bars: 40 µm. (**C-F**) Mean pixel intensity within these ROIs was measured at each time point in XYZT time-lapse movies collected at 5 min intervals. The CSF tracer moved readily into the cortex along penetrating arterioles and into the brain parenchyma in the sleeping and anesthetized state (green and red lines), but not in awake mice (orange line; *$p < 0.05$, $n = 6$ each group). **(G)** Radio labeled ^{3}H-mannitol was injected intracisternally in awake and anesthetized mice. Brains were harvested 15, 30 or 45 min after radio-tracer injection to quantify radiotracer accumulation within the brain parenchyma. Brains were solubilized in Soluene, and total brain count was detected by liquid scintillation counting. Total ^{3}H counts from brain divided by total injected ^{3}H-mannitol were used to calculate CSF influx (*3*). ^{3}H-mannitol accumulated gradually in brain with time in mice anesthetized with ketamine/xylazine, but not significantly in awake mice (*$p < 0.05$, $n = 4$-6 each group, 2-way ANOVA with Bonferroni's post-hoc test).

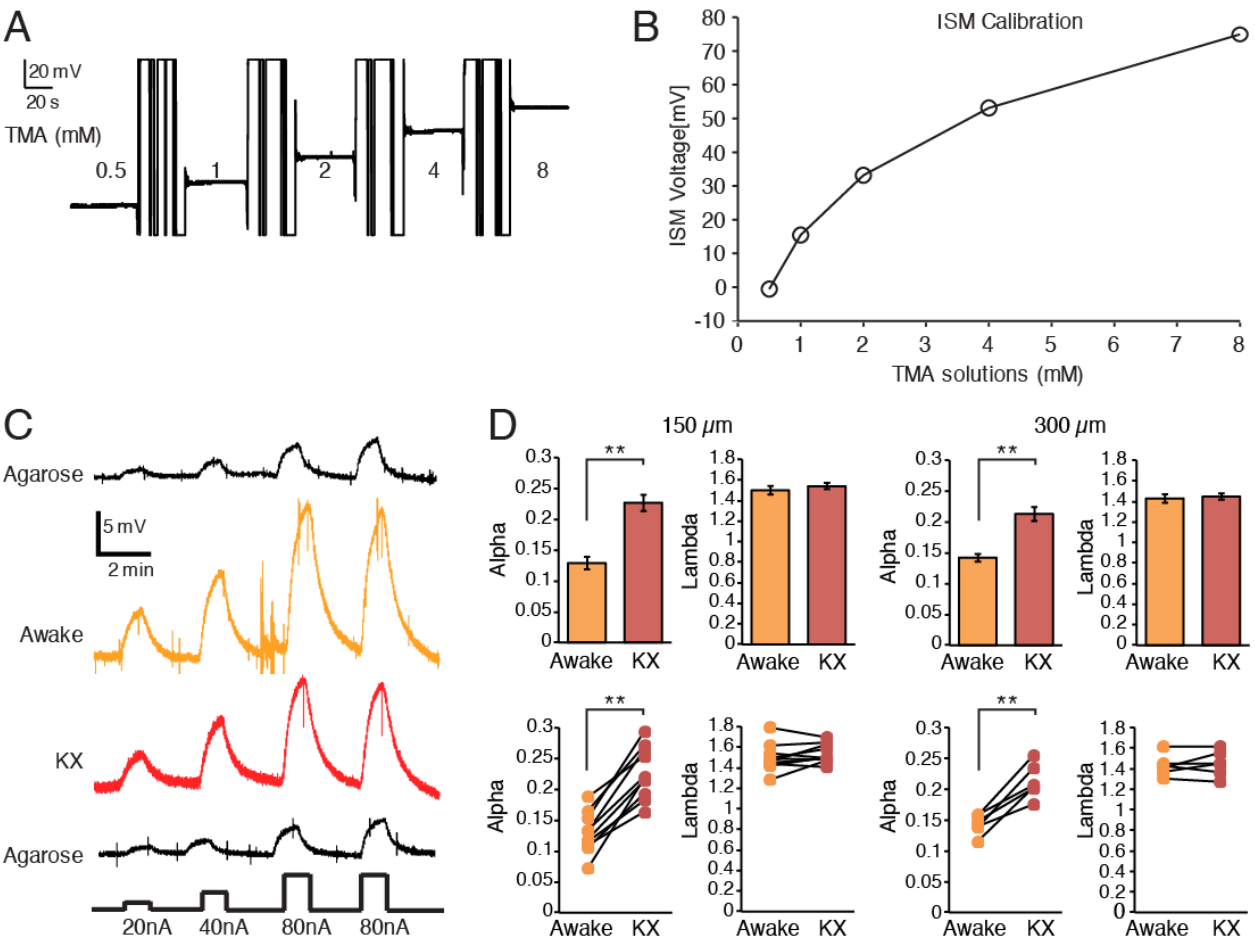

Fig. S3. Measurement of interstitial space volume fraction and tortuosity using the iontophoretic TMA^+ method

(A) TMA-ion selective microelectrodes (ISMs) were calibrated in aCSF solution containing 0.5, 1, 2, 4, and 8 mM TMA-chloride. **(B)** The voltage *versus* the TMA^+ concentration was plotted and fitted to Nikolsky equation (*16*). (**C**) Representative examples of TMA^+ diffusion curves from one experiment in which recordings were first obtained in 1) agorose, 2) awake mouse (150 µm below the cortical surface), 3) same mouse after administration of ketamine/Xylazine (without moving the electrodes), and 4) agarose. Four current injections (20, 40, 80, and 80 nA) were analyzed. (**D**) Alpha and lambda collected at a depth of 150 *versus* 300 µm below the cortical surface did not differ significantly in either the awake or the ketamine/xylazine anesthetized state (n = 10 for 150 µm, n = 6 for 300 µm; ** $p < 0.01$, paired t test).

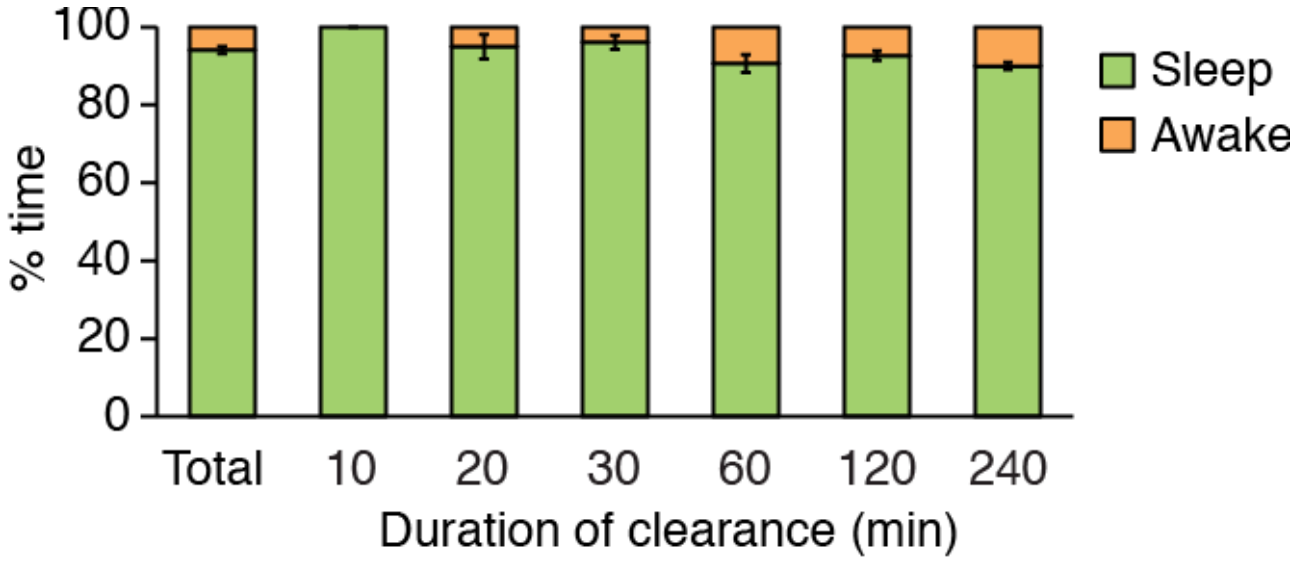

Fig. S4. Sleep scoring for clearance studies

Recordings of ECoG and EMG were not obtained in radiolabeled clearance studies to avoid contaminating the equipment. Instead animals in the awake group were kept alert during the experiments by gentle movement of their cages. Clearance data for sleep was obtained by keeping the room quiet, while an immobilized observer scored the activity state of the mice (sleep versus awake) every 5 min throughout the experiments. The relative amount of sleep in the sleep group during clearance was calculated and plotted. None of the animals in the ketamine/xylazine woke up during the clearance phase (n = 4-27, P = 0.06, one way ANOVA.)

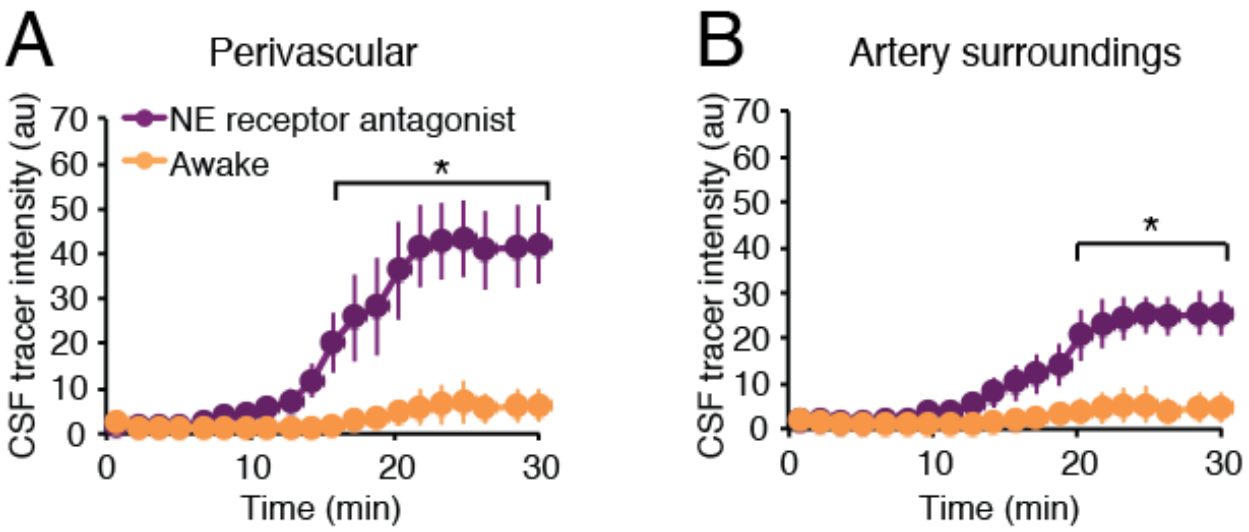

Fig. S5. Intracisternal administration of a mixture of norepinephrine receptor antagonists increases CSF tracer influx.

A mixture of norepinephrine receptor antagonists (prazosin, atipamezole and propranolol, each 2 mM), was injected into the cisterna magna of awake mice starting with a bolus of 5 µl (1µl/min) followed by a constant infusion of 0.167µl/min with a syringe pump until the end of experiment. Using the same approach to detect influx of CSF tracers shown in Fig. S2, the kinetics of tracer influx were compared before and 15 min after NE receptor antagonist administration. Influx of the two dextrans of same molecular weight (TR-d3 and FITC-d3) injected in awake mice orange line prior to administration of norepinephrine receptor antagonists and again 15 min after the injection of the norepinephrine receptor antagonists (purple line) were calculated along peri-arterial pathways and in the cortical parenchyma (*p < 0.05, n= 6 each group, two-way ANOVA with Bonferroni test).